RESEARCH ARTICLE | NOVEMBER 01 1993

Elliptical instability in a stably stratified rotating fluid

Takeshi Miyazaki

Phys. Fluids 5, 2702–2709 (1993)
https://doi.org/10.1063/1.858733

Elliptical instability in a stably stratified rotating fluid

Takeshi Miyazaki
Department of Mechanical and Control Engineering, University of Electro-Communications, Chofu, Tokyo 182, Japan

(Received 13 January 1993; accepted 17 May 1993)

The linear stability of unbounded strained vortices in a stably stratified rotating fluid is investigated theoretically. The problem is reduced to a Matrix–Floquet problem, which is solved numerically to determine the stability characteristics. The Coriolis force and the buoyancy force suppress the subharmonic elliptical instability of cyclonic and weak anticyclonic vortices, whereas enhances that of strong anticyclonic vortices. The fundamental and superharmonic instability modes occur, in addition. They are due to higher-order resonance. The growth rate of each instability shows complicated dependence on the parameters N (the normalized Brunt–Väisälä frequency) and R_0 (the Rossby number: defined inversely as usual), if their values are small. It decreases as the background rotation rate becomes larger and as the stratification becomes stronger. The instability mode whose order of resonance is less than $\mathrm{Min}(N,2|1+R_0|)$ is inhibited.

I. INTRODUCTION

There have been extensive investigations on the motion and stability of concentrated vortices, which appear in high Reynolds number flows as coherent structures. Recently, Pierrehumbert[1] showed numerically that an unbounded inviscid strained vortex undergoes instability whose growth rate is independent of wavelength. Bayly[2] formulated the problem as a matrix Floquet problem, which indicated that the instability mode is parametrically excited. Waleffe[3] reduced the problem to an Ince equation and explored its analytical structure thoroughly. He gave, in the limiting case of weak strain, a lucid physical explanation of the instability as a resonant interaction between the inertial wave and the imposed strain field. This broadband instability is called the elliptical instability and it constitutes the essential part of the classical short-wave instability of concentrated vortices in a locally imposed strain field.[4–7] The continuous instability mode is discretized to be reducible to the W–B–T instability modes,[8] if an appropriate outer boundary condition is taken into account. Gledzer and Ponomarev[9] investigated the instability of a solid body rotation of fluid in an elliptical cylinder and compared their results with the predictions of the elliptical instability. It is not difficult to incorporate the viscous effect, which was undertaken by Landman and Saffman.[10] They showed that this intrinsically inviscid instability mechanism persists even in the presence of the viscous dissipation.[11]

Atmospheric and oceanographic fluid motions are subjected to a strong influence both of the Coriolis force due to the earth's rotation and of the buoyancy force associated with temperature and/or salinity variations. Craik[12] proposed to incorporate the contribution of these types of body force and described the influence of the Coriolis force in detail. The elliptical instability is weakened for cyclonic vortices ($\mathrm{Ro}>0$) and for weak anticyclonic vortices ($\mathrm{Ro}<-1$), where Ro denotes the Rossby number defined inversely as usual. The instability is enhanced for strong anticyclonic vortices ($-1<\mathrm{Ro}<0$), where disturbances in a horizontal plane grow. Gledzer and Ponomarev[9] considered the Coriolis effect in their experiment and good agreement with the result by Craik[12] was obtained. Miyazaki and Fukumoto[13] investigated the effect of stable stratification on the elliptical instability. (Gledzer and Ponomarev[9] mentioned the same issue, but they did not give detailed discussions.) The elliptical instability of Pierrehumbert type (the subharmonic mode) is suppressed and disappears when the Brunt–Väisälä frequency N exceeds unity. On the other hand, the fundamental and superharmonic instability modes are found to occur as the result of resonant excitation of inertial gravity waves. The fundamental mode is presented when the Brunt–Väisälä frequency is less than 2, whereas the superharmonic modes persist for any nonzero Brunt–Väisälä frequency. Our objective in this paper is to explore the combined effect of these body forces on the elliptical instability, when both of them are presented.

We formulate the problem in Sec. II, where it is reduced to a Matrix–Floquet problem. The fluid is assumed to be inviscid, incompressible, nondiffusive. It is exponentially stratified in the vertical direction and subjected to a uniform background rotation around the vertical axis. Since we consider the instability modes induced near the center of a strained vortex, the centrifugal force due to vortex motion (and due to the coordinates' rotation) is assumed to be very weak compared to the gravity. Then, an approximation similar to the Boussinesq approximation is introduced. The Floquet problem is solved numerically. The influence of the Coriolis force is reviewed in Sec. III, briefly. Some new findings, such as the occurrence of superharmonic instabilities, are added to Craik's results. Although the growth rate of superharmonic mode is very small compared with that of the subharmonic instability and the instability band is very narrow, they become evident, if the stratification effect is incorporated. Our main results are described in Sec. IV. It is shown that both effects suppress the subharmonic instability but that the fundamental and superharmonic instabilities occur. The growth rate of each mode becomes smaller as the back-

 0899-8213/93/5(11)/2702/8/$6.00

ground rotation rate becomes larger and the stratification becomes stronger. The instability mode due to resonance whose order is less than $\mathrm{Min}[N,2|1+R_0|]$, is inhibited. The last section is devoted to summary and discussions.

II. FORMULATION

The fluid is assumed to be inviscid, incompressible, and nondiffusive. The equations of motion in the coordinates rotating with the angular velocity $\mathbf{\Omega e}_z$ are written in vector form as

$$\rho\left(\frac{\partial \mathbf{u}}{\partial t}+\mathbf{u}\cdot\mathrm{grad}\,\mathbf{u}+2\mathbf{\Omega e}_z\times\mathbf{u}\right)=-\mathrm{grad}\,p-\rho g\mathbf{e}_z, \quad (1)$$

where $\mathbf{u}=u\mathbf{e}_x+v\mathbf{e}_y+w\mathbf{e}_z$ is the velocity field and ρ and p denote the density and pressure, respectively. The Cartesian coordinates (x,y,z) are used throughout this paper with the corresponding unit vectors $\mathbf{e}_x$, $\mathbf{e}_y$, and $\mathbf{e}_z$. The gravity g acts in the negative z direction. The conditions of incompressibility and nondiffusivity impose

$$\frac{\partial \rho}{\partial t}+\mathbf{u}\cdot\mathrm{grad}\,\rho=0. \quad (2)$$

In consequence, the velocity becomes solenoidal:

$$\mathbf{div}\,\mathbf{u}=0. \quad (3)$$

A. Basic state

The density is assumed to be exponentially stratified in the z direction, so that the Brunt–Väisälä frequency $N^2=\alpha g/\gamma^2$ is a constant throughout the entire fluid. Here α is the exponent of stable stratification and 2γ denotes the uniform vertical vorticity. The centrifugal force associated with vortex motion is assumed to be weak compared with the gravity, as in Miyazaki and Fukumoto.[13] This ratio is characterized by the Froude number $\mathrm{Fr}=\gamma^2L/g$, where L denotes the length scale within which the following linear velocity profiles are thought of as a good approximation. In other words, we base our approach on the Wentzel–Kramers–Brillouin method (implicitly) which was introduced, explicitly, by Lifschitz[14] and Lifschitz and Hameiri[15] in the discussions on local stability conditions. We seek for the steady basic state in the following form of expansions in powers of the small parameter $N^2\mathrm{Fr}^2$:

$$U=-\gamma L[(1+\epsilon)y+O(N^2\mathrm{Fr}^2)], \quad (4)$$

$$V=\gamma L[(1-\epsilon)x+O(N^2\mathrm{Fr}^2)], \quad (5)$$

$$W=\gamma LN^2\mathrm{Fr}[W_1(x,y)+O(N^2\mathrm{Fr}^2)], \quad (6)$$

$$\rho_0=\rho^* e^{-\alpha Lz}[1+N^2\mathrm{Fr}^2\rho_1(x,y)+O(N^4\mathrm{Fr}^4)], \quad (7)$$

$$P=\frac{\rho^* g}{\alpha}e^{-\alpha Lz}[1+N^2\mathrm{Fr}^2p_1(x,y)+O(N^4\mathrm{Fr}^4)], \quad (8)$$

where the space coordinates (x,y,z) are normalized by L and the time by $1/\gamma$. The strength of the rate of strain is represented by ϵ (<1). The quantities with the subscript 1 are determined, after substituting (4)–(8) into (1) and (2), as

$$p_1=\left(\frac{1-\epsilon^2+R_0^2}{2}\right)(x^2+y^2)+R_0[(1-\epsilon)x^2+(1+\epsilon)y^2], \quad (9)$$

$$\rho_1=R_0[(1-\epsilon)x^2+(1+\epsilon)y^2]+\frac{1-\epsilon^2+R_0^2}{2[N^2-4(1-\epsilon^2)]}\times[(N^2-4+4\epsilon)x^2+(N^2-4-4\epsilon)y^2], \quad (10)$$

$$W_1=-\frac{2\epsilon(1-\epsilon^2+R_0^2)}{N^2-4(1-\epsilon^2)}xy, \quad (11)$$

Here, $\mathrm{Ro}=\Omega/\gamma$ denotes the Rossby number defined inversely as usual for later convenience. The Rossby number is positive for cyclonic eddies and negative for anticyclonic eddies. Its magnitude increases as the vortex becomes weak and as the background rotation becomes strong. It is noted that (10) and (11) diverge at $N=2(1-\epsilon^2)^{1/2}$. The divergence takes place when a fluid particle oscillates (with the Brunt–Väisälä frequency) vertically, just twice during it moves around the vortex center once. Miyazaki[16] studied similar resonance phenomena for general vorticity distributions, incorporating weak viscous effect. It was shown that an internal boundary layer is formed when the resonance condition is satisfied. We will see later that the same resonance is related to the fundamental instability, but we must keep in mind that our approximation deteriorates in the vicinity of the critical line $N^2=4(1-\epsilon^2)$, because we fail to construct the basic state in our (inviscid) framework.

B. Linear disturbances

We consider the linear stability of the above basic state under the assumption of weak centrifugal force. The nondimensional velocity disturbances (u',v',w') and the density ρ' and the pressure perturbation p' are introduced as follows:

$$u=U+\gamma Lu', \quad (12)$$

$$v=V+\gamma Lv', \quad (13)$$

$$w=W+\gamma Lw', \quad (14)$$

$$\rho=\rho_0+\rho^* e^{-\alpha Lz}N^2\mathrm{Fr}\rho', \quad (15)$$

$$p=P+\rho^*\gamma^2L^2e^{-\alpha Lz}p'. \quad (16)$$

Substituting (12)–(16) into (1)–(3) and discarding nonlinear terms, as well as the higher-order terms in the Fr expansion, we have the following set of linearized equations:

$$D_tu'-(1+\epsilon)v'-2R_0v'=-\frac{\partial p'}{\partial x}, \quad (17)$$

$$D_tv'+(1-\epsilon)u'+2R_0u'=-\frac{\partial p'}{\partial y}, \quad (18)$$

$$D_t w' = -\frac{\partial p'}{\partial z} - N^2 \rho', \tag{19}$$

$$D_t \rho' - w' = 0, \tag{20}$$

$$\text{div } \mathbf{u}' = 0, \tag{21}$$

where D_t denotes the Lagrangian derivative along the basic flow field,

$$D_t \equiv \frac{\partial}{\partial t} - (1+\epsilon) y \frac{\partial}{\partial x} + (1-\epsilon) x \frac{\partial}{\partial y}. \tag{22}$$

Let us consider the disturbances in the form of plane wave with time dependent wave number as Bayly,[2] Landman and Saffman,[10] Waleffe,[3] and Craik[12] [Craik and Criminale[17] demonstrated that the solutions of following form provide a new class of three-dimensional (3-D) exact solutions of the Navier–Stokes equations under a more general situation]:

$$\begin{pmatrix} u' \\ v' \\ w' \\ \rho' \end{pmatrix} = \begin{pmatrix} \hat{u} \\ \hat{v} \\ \hat{w} \\ \hat{\rho} \end{pmatrix} e^{i\mathbf{k}(t)\cdot\mathbf{x}}, \tag{23}$$

where

$$k_x = \sin\theta \cos\varphi,$$

$$k_y = (1+\epsilon)^{1/2}(1-\epsilon)^{-1/2} \sin\theta \sin\varphi, \quad k_z = \cos\theta, \tag{24}$$

and

$$\varphi = (1-\epsilon^2)^{1/2} t. \tag{25}$$

As the problem is scale independent, the wave number $\mathbf{k}$ is characterized by an angle parameter θ and φ denotes the renormalized time variable. Substitution of (23)–(25) into (17)–(21) and elimination of p' and w', yield the equation describing the time evolution of the disturbance–amplitude $(\hat{u},\hat{v},\hat{\rho})$:

$$\sqrt{1-\epsilon^2}\frac{d\hat{u}}{d\varphi} = (1+\epsilon+2R_0)\hat{v} + \frac{k_x}{k^2}[2(1+R_0)(k_y\hat{u}-k_x\hat{v}) - 2\epsilon(k_y\hat{u}+k_x\hat{v}) + N^2 k_z\hat{\rho}], \tag{26}$$

$$\sqrt{1-\epsilon^2}\frac{d\hat{v}}{d\varphi} = -(1-\epsilon+2R_0)\hat{u} + \frac{k_y}{k^2}[2(1+R_0)(k_y\hat{u}-k_x\hat{v}) - 2\epsilon(k_y\hat{u}+k_x\hat{v}) + N^2 k_z\hat{\rho}], \tag{27}$$

$$\sqrt{1-\epsilon^2}\frac{d\hat{\rho}}{d\varphi} = -\frac{1}{k_z}(k_x\hat{u}+k_y\hat{v}), \tag{28}$$

with $k^2 = k_x^2 + k_y^2 + k_z^2$. Thus the problem is reduced to a 3×3 Matrix–Floquet problem.

We calculate the Floquet multipliers ν_i, by integrating (26)–(28) numerically from 0 to 2π (the fouth-order Runge–Kutta–Gill method) and by determining the eigenvalues of the solution matrix numerically (double QR method). We notice that one multiplier ν_3 (say) is unity and that the others ν_1, ν_2 satisfy the relation $\nu_1 \cdot \nu_2 = 1$,

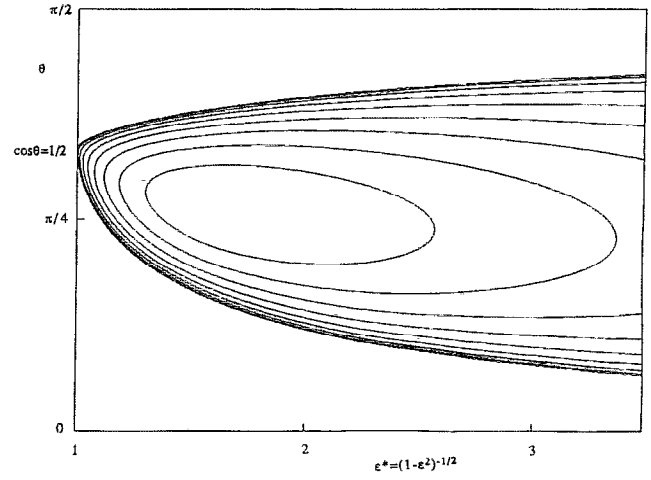

FIG. 1. Contour maps of the growth rate σ for $N=0.0$. The horizontal axis denotes the renormalized strain rate ϵ^* and the vertical axis is the angle θ of the wave number to the vertical direction. The outermost line traces the growth rate 10^{-5}, and the contour interval is 0.04.

with ν_i being complex conjugates of each other or real reciprocals. When the latter happens, the proper choice of growth rate is

$$\sigma = \frac{\sqrt{1-\epsilon^2}}{2\pi} \log|\nu_1|, \tag{29}$$

where ν_1 is the multiplier with larger absolute value.

III. EFFECTS OF THE CORIOLIS FORCE

We review the Craik's results for a homogeneous rotating fluid[12] ($N=0$) in this section, supplying some new information. Figure 1 depicts the contours of constant growth rate in the $\epsilon^*-\theta$ plane for the nonrotating case (Ro=0). The horizontal axis is related to the rate of strain ϵ by $\epsilon^* = (1-\epsilon^2)^{-1/2}$ and the vertical one denotes the angle θ between the wave-number vector and the vertical axis (at the initial time). The parameter ϵ^* is proportional to the time period in which a fluid particle moves around the vortex center. This parameter is more convenient than ϵ in order to observe resonance phenomena, later. The outermost contour traces the growth rate 10^{-5} and the inner lines correspond to the levels of 0.04, 0.08, 0.12, etc. Of course, it is the elliptical instability of Pierrehumbert type (the subharmonic instability). In the weak strain limit, the instability region touches the θ axis at $\theta_1 = \pi/3$, where the resonance between the inertial wave and the imposed strain field occurs.[3] Since the Coriolis force changes the dispersion relation of inertial waves, the elliptical instability suffers substantial influence, too.

The effects of the Coriolis force are illustrated in Figs. 2–5. Each figure shows the contours of constant growth rate. The contour levels are the same as in Fig. 1. The values of the Rossby number are 0.6 (Fig. 2), −0.6 (Fig. 3), −1.3 (Fig. 4), and −2.3 (Fig. 5).

We see in Fig. 2 that the cyclonic background rotation works in the direction to suppress the subharmonic instability mode, as Craik[12] demonstrated. The instability

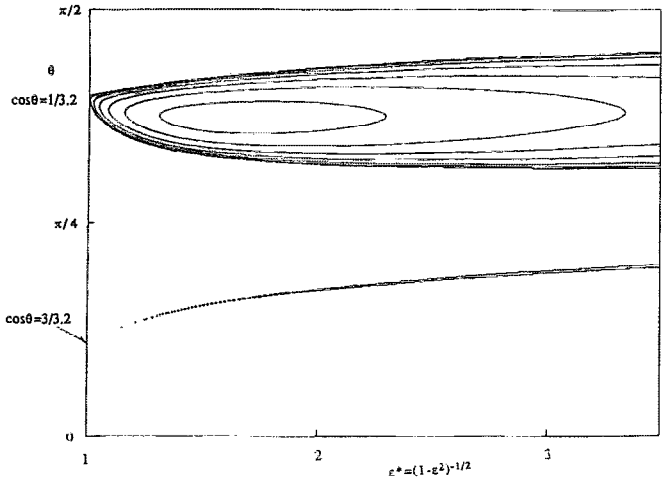

FIG. 2. Contour maps of the growth rate σ for Ro=0.6. The axes and the contour levels are the same as in Fig. 1.

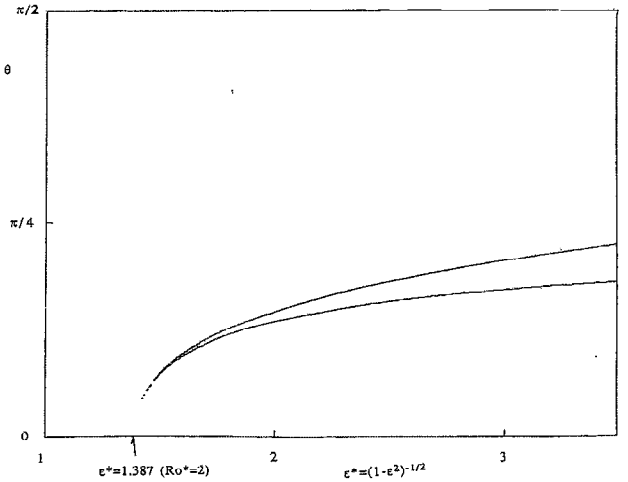

FIG. 4. Contour maps of the growth rate σ for Ro$=-1.3$. The axes and the contour levels are the same as in Fig. 1.

branch reaches the θ axis at $\theta_1=\cos^{-1}[0.5/(1+\mathrm{Ro})]$, reflecting the fact that the resonance condition is modified under the influence of the Coriolis force. The suppression becomes more evident and the parameter region of instability moves further upward as Ro is increased, but the subharmonic instability does not disappear. It is also noted that a narrow instability branch manifests itself. It seems to reach the θ axis at $\theta_3=\cos^{-1}[1.5/(1+\mathrm{Ro})]$, indicating the occurrence of a superharmonic instability of the third order. Since it is very weak and its parameter region is very narrow (the small "islands" and the small-scale waviness of the lowest contour, in Fig. 2 and subsequent figures, are artifacts of the contouring routine), it is understandable that Craik[12] did not refer to the occurrence of superharmonic modes. They may have little importance under the existence of the subharmonic instability mode that is much stronger. They become, however, evident if the effect of stable stratification is incorporated, since, then, the subharmonic instability vanishes.

Figure 3 shows that the subharmonic instability is enhanced for strong anticyclonic vortices ($-1<\mathrm{Ro}<0$). It is due to the destabilization of horizontal ($\theta=0$) disturbances, whose mechanism can be understood easily from Eqs. (17) and (18) [or from (26) and (27)] by putting the right-hand side terms to be zero. They represent exponential growth of disturbances for $\epsilon>|1+2\mathrm{Ro}|$, indicating that a highly strained vortex is strongly unstable. When $\epsilon<|1+\mathrm{Ro}|$, these equations describe a stable horizontal ($\theta=0$) oscillation of period $\sqrt{(1+2R_0)^2-\epsilon^2}$ (the inertial wave). This inertial wave can, again, cause instability through resonance between the imposed strain field. We see in Fig. 4 that the subharmonic instability branch stretches toward the ϵ^* axis and seems to touch it at $\mathrm{Ro}^*=\epsilon^*\sqrt{(1+2R_0)^2-\epsilon^2}=2$. Here, Ro* denotes the renormalized (by the period of vortex rotation) frequency of the inertial oscillation.

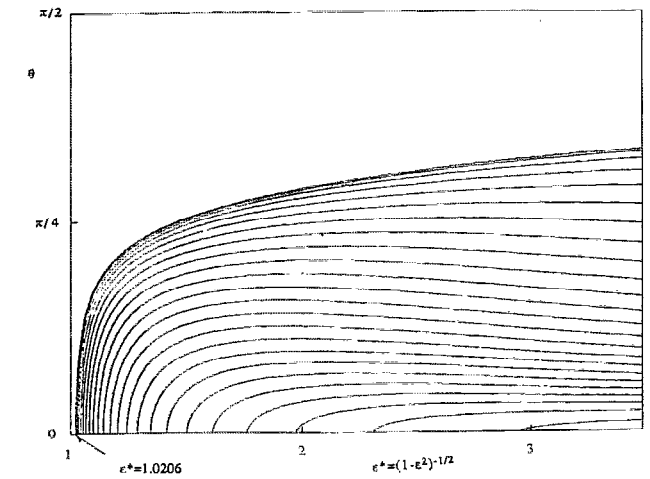

FIG. 3. Contour maps of the growth rate σ for Ro$=-0.6$. The axes and the contour levels are the same as in Fig. 1.

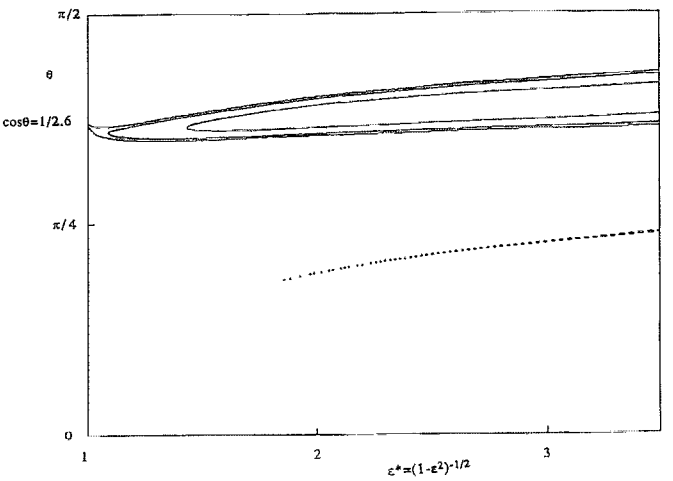

FIG. 5. Contour maps of the growth rate σ for Ro$=-2.3$. The axes and the contour levels are the same as in Fig. 1.

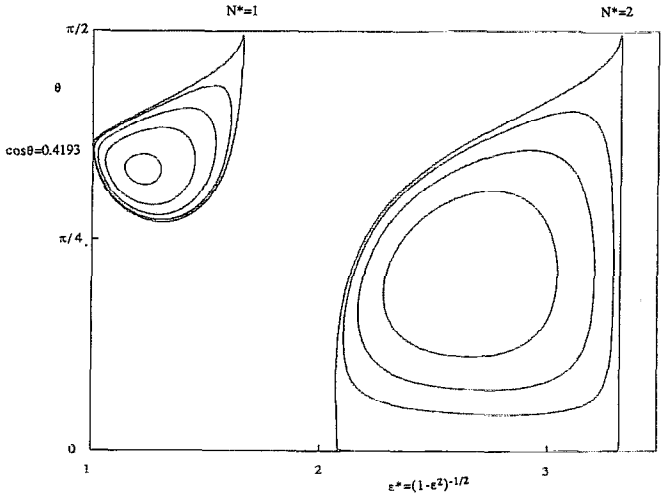

FIG. 6. Contour maps of the growth rate σ for $N=0.6$. The axes and the contour levels are the same as in Fig. 1.

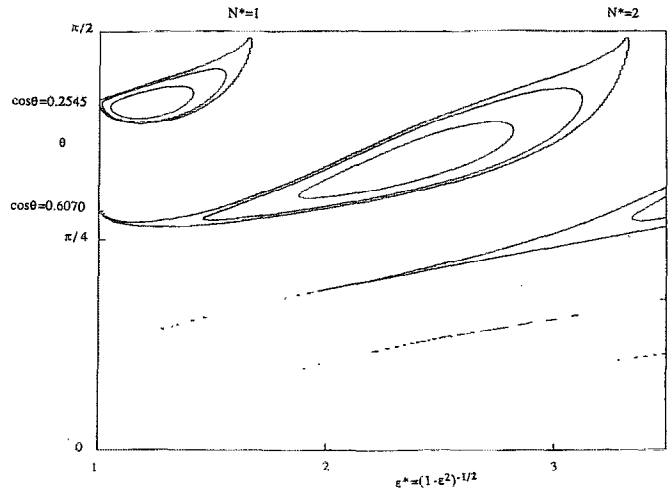

FIG. 8. Contour maps of the growth rate σ for $(N,\mathrm{Ro})=(0.6,0.6)$. The axes and the contour levels are the same as in Fig. 1.

As the vortex becomes weaker (i.e., as Ro decreases less than -1.5), the stability characteristics become similar to those of cyclonic vortices. We observe the subharmonic and superharmonic instability modes in Fig. 5. Each instability branch reaches the ϵ^* axis at $\mathrm{Ro}^*=$an integer or touches the θ axis at $2(1+\mathrm{Ro})\cos\theta=$an integer. The elliptical instability is weakened by the Coriolis effect, if the vorticity of the vortex is small compared with the background vorticity.

IV. EFFECTS OF STABLE STRATIFICATION

This section illustrates our main findings, i.e., the influence of stable stratification on the elliptical instability. First, we give a few comments on the nonrotating ($\mathrm{Ro}=0$) case, which was considered by Miyazaki and Fukumoto.[13] Figures 6 and 7 show the contour maps of the growth rate for $N=0.6$ and $N=1.5$, respectively. They are identical to Figs. 3 and 5 in Miyazaki and Fukumoto,[13] except for the difference of the horizontal axis ϵ^* (in place of ϵ) and the refined resolution. The subharmonic instability is suppressed and its parameter region is limited from right by the line $\epsilon^*=1/N$ ($N^*=N\epsilon^*=1$) and then it disappears when the Brunt–Väisälä frequency N exceeds unity (Fig. 7). On the other hand, we find in Fig. 6 that the fundamental instability mode extends to the left side of the critical line $\epsilon^*=2/N$ ($N^*=2$), which corresponds to the condition of the parametric excitation of buoyancy oscillation. The instability region between the θ axis and the vertical line $\epsilon^*=2/N$ shrinks as N increases, and the fundamental instability disappears for $N>2$. Three superharmonic instability modes are observed in Fig. 7. The instability branches touch the upper horizontal line $\theta=\pi/2$ at $N^*=3$, 4 and 5, respectively. It is why we call them the "superharmonic" instabilities.[13] They emanate from the lower right corner $(\epsilon^*,\theta)=(\infty,0)$. There are infinite number of superharmonic branches corresponding to integers larger than 2, for any positive N. Only the superharmonic instability modes survive for N larger than 2.

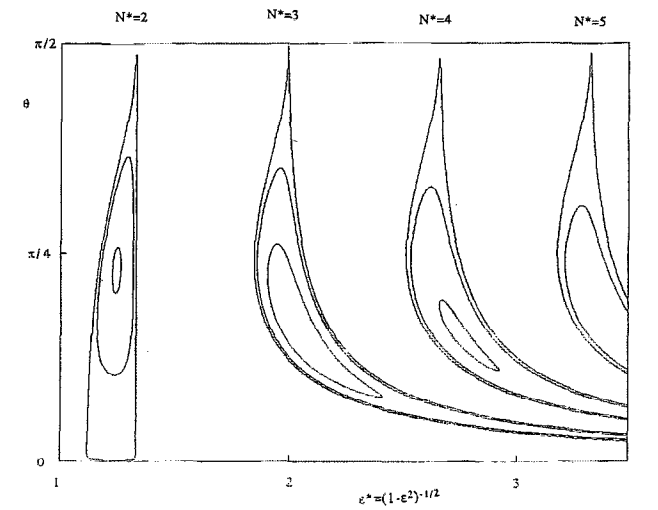

FIG. 7. Contour maps of the growth rate σ for $N=1.5$. The axes and the contour levels are the same as in Fig. 1.

There are two characteristic features of the elliptical instability under a stable stratification. First, each instability branch reaches the line $\theta=\pi/2$ at $N^*=$(an integer) or touches the θ axis at $N^2+(4-N^2)\cos^2\theta=$(an integer)^2. Second, the subharmonic and the fundamental modes (two instability modes associated with lower-order resonance) disappear as the Brunt–Väisälä frequency increases. Our next concern is the combined effects of the background rotation and the stable stratification.

Figures 8–10 show the contour levels of the growth rate for cyclonic vortices, where the parameters (Ro, N) are (0.6, 0.6), (0.6, 1.5) and (0.3, 1.5), respectively. We see the subharmonic, fundamental, and superharmonic instabilities in Fig. 8, whereas only the fundamental and superharmonic modes in Fig. 9. As N increases, the upper attaching point ($N^*=$an integer) of each instability branch moves in the left with the lower attaching point

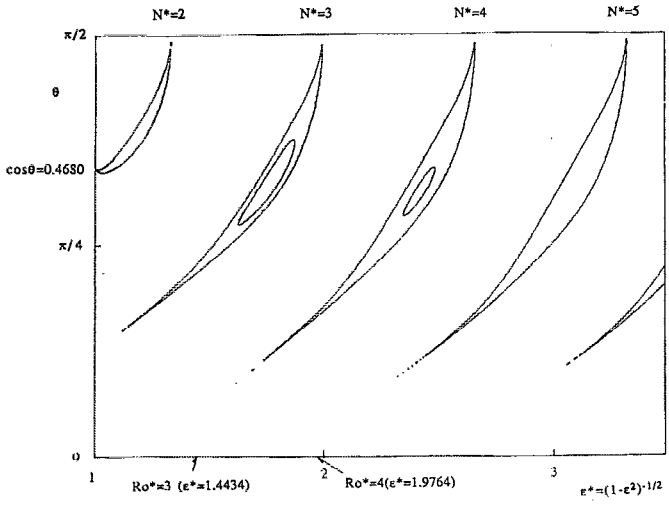

FIG. 9. Contour maps of the growth rate σ for $(N,\mathrm{Ro})=(1.5,0.6)$. The axes and the contour levels are the same as in Fig. 1.

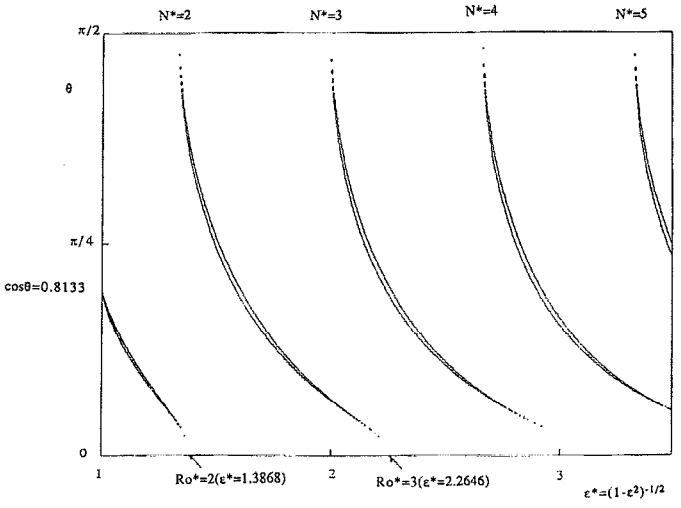

FIG. 11. Contour maps of the growth rate σ for $(N,\mathrm{Ro})=(1.5,-1.3)$. The axes and the contour levels are the same as in Fig. 1.

(Ro*=an integer) being fixed. Conversely, if we fix the Brunt–Väisälä frequency N and change the Rossby number Ro, the lower attaching point moves with the upper point being fixed (compare Figs. 9 and 10). The correspondence between the upper attaching point and the lower one is given by the relation $N^*=\mathrm{Ro}^*+1=I$, where I denotes the order of resonance. The lower point $\mathrm{Ro}^*=I-1$ reaches the θ axis when $\mathrm{Ro}=(I-2)/2$, then the Ith instability branch touches the θ axis at $N^2\sin\theta_I+4(1+\mathrm{Ro})^2\cos^2\theta_I=I^2$ for $\mathrm{Ro}>(I-2)/2$. Similarly, the upper attaching point $N^*=I$ reaches the θ axis when $N=I$. We notice from these observations that the instability mode whose resonance order is less than $\mathrm{Min}[N,2(\mathrm{Ro}+1)]$, is inhibited. It is notable that any instability mode may disappear depending on the values of N and R_0 under the presence of both effects, while only the subharmonic and fundamental modes disappear under the influence of stratification alone. We can judge, roughly, whether a certain strained vortex (ϵ_0) under the background rotation (Ro) and the stable stratification (N) is stable or not and to what mode it becomes unstable if it is unstable, only by drawing lines connecting the corresponding points, i.e., $\mathrm{Ro}^*=I-1$, $N^*=I$, and $\theta=\theta_I$ for various resonance order I. If the vertical line $\epsilon^*=\epsilon_0^*$ crosses some of these lines the vortex is known to be unstable, conversely, if there is no cross point the vortex may be stable. Of course, more detailed discussions are required, if the instability bands are fat.

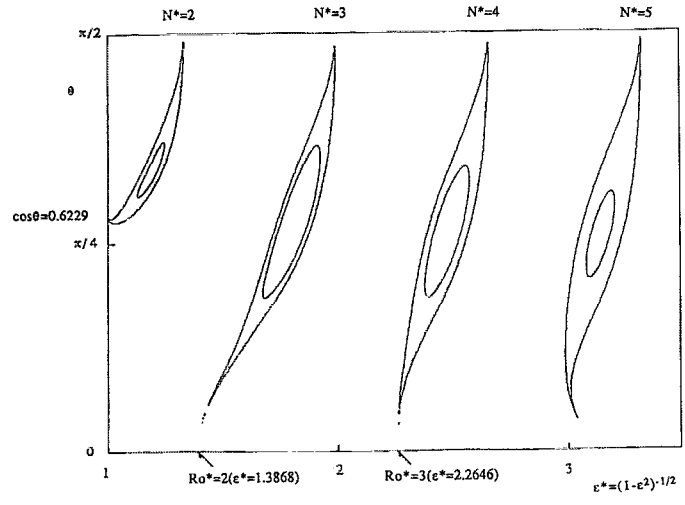

FIG. 10. Contour maps of the growth rate σ for $(N,\mathrm{Ro})=(1.5,0.3)$. The axes and the contour levels are the same as in Fig. 1.

Similar instability characteristics are observed for weak anticyclonic vortices. The Ith instability branch reaches the upper line $\theta=\pi/2$ at $N^*=I$ and the ϵ^* axis at $\mathrm{Ro}^*=I+1$. Figure 11 shows the contour maps for $(N,\mathrm{Ro})=(1.5,-1.3)$. There are the subharmonic, fundamental, and superharmonic instability branches. The lower attaching point of the Ith mode reaches the θ axis when $\mathrm{Ro}=(-1-I)/2$. In this case, the above statement concerning the disappearance of instability mode holds again, if we replace $2(\mathrm{Ro}+1)$ by $2(-\mathrm{Ro}-1)$.

The behavior of strong anticyclonic vortices ($-1<\mathrm{Ro}<0$) is somewhat different from that of cyclonic and weak anticyclonic vortices. Figure 12 shows the contour maps for $(N,\ \mathrm{Ro})=(0.6,\ -0.6)$. Since the instability modes in the horizontal plane ($\theta=0$) are not affected by the stable stratification, the elliptical instability is not suppressed and all modes (subharmonic, fundamental, and superharmonic) are presented. It is notable that the stratification does enhance the instability of weakly strained vortices in the parameter range $-1<\mathrm{Ro}<-0.5$ (compare Figs. 3 and 12).

Thus the stable stratification has nontrivial effects on the elliptical instability, especially when it is combined with the background rotation (the Coriolis effect). The growth rate of each instability mode shows complicated dependence on the parameters N and Ro when their absolute values are small or moderate, but it decreases rapidly as N and Ro are increased further. The quasigeostrophic

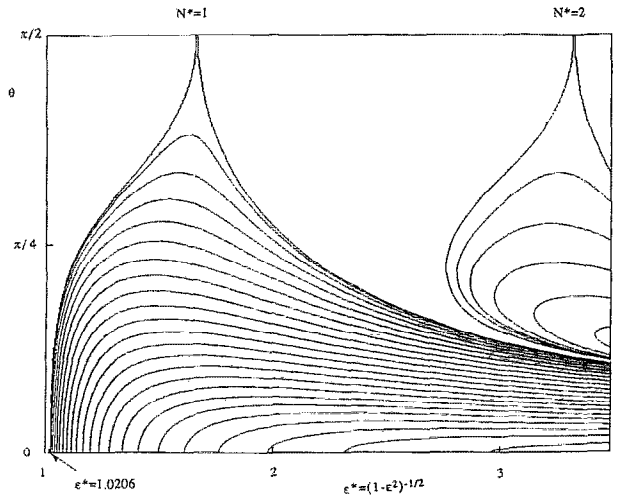

FIG. 12. Contour maps of the growth rate σ for $(N, \mathrm{Ro})=(0.6, -0.6)$. The axes and the contour levels are the same as in Fig. 1.

approximation is introduced in order to describe large-scale geophysical fluid motions efficiently, i.e., in the limit of large background rotation and strong stable stratification. It is demonstrated in the appendix that no elliptical instability occurs for a quasigeostrophic vortex motion, where the hydrostatic balance is assumed. We should keep in mind this limitation of the quasigeostrophic approximation in applying it to a specific case.

V. SUMMARY AND DISCUSSIONS

In this paper, we have clarified the effects of the Coriolis and buoyancy force on the elliptical instability of strained vortices. The fluid is assumed to be inviscid, incompressible, and nondiffusive. It is exponentially stratified and subjected to a uniform background rotation.

The subharmonic elliptical instability (Pierrehumbert–Bayly type) of cyclonic ($\mathrm{Ro}>1$) and weak ($\mathrm{Ro}<-1$) anticyclonic vortices is shown to be suppressed by the Coriolis and stratification effects, whereas the fundamental and the superharmonic modes are found to occur. The growth rate of a higher-order instability mode, first, increases as the Brunt–Väisälä frequency N is increased, but it decreases as N increases further. The instability of the order lower than $\mathrm{Min}[N, 2|1+\mathrm{Ro}|]$ is inhibited. Since even a weak viscous dissipation, which can be incorporated easily in the stability analysis,[10] will suppress weak short-wave instabilities, cyclonic and weak anticyclonic vortex structures in a strongly stratified and rapidly rotating fluid may, in effect, be stable to any 3-D disturbances.

All instability modes are presented for strong ($-1<\mathrm{Ro}<0$) anticyclonic vortices under a stable stratification. The growth rate of disturbances in a horizontal plane ($\theta=0$ mode) are not affected by the stratification. It is remarkable that the stratification even enhances the elliptical instability (in $\theta>0$ parameter region), in this case.

We have revealed in this paper that the body forces, such as the Coriolis and buoyancy force, have substantial effects on the elliptical instability of strained vortices, especially when they are combined. It is because the dispersion relation of inertial gravity waves are modified under the influence of these body forces and so are the resonance conditions. Although our study is limited to the highly idealized case, it will provide some insights in the understanding of geophysical fluid motions.

APPENDIX: ELLIPTICAL INSTABILITY OF QUASIGEOSTROPHIC VORTICES

This appendix illustrates that no elliptical instability is presented under the f-plane quasigeostrophic approximation, which is thought of a good approximation in the limiting case of large Brunt–Väisälä frequency N and large Rossby number Ro (or small Rossby number in the usual definition). The f-plane quasigeostrophic equation

$$\left(\frac{\partial}{\partial t}+\frac{\partial\psi\partial}{\partial y\partial x}-\frac{\partial\psi\partial}{\partial x\partial y}\right)(\Delta+L_z)\psi=0 \tag{A1}$$

has the following two-dimensional steady solution:

$$\psi=-\tfrac{1}{2}[(1+\epsilon)y^2+(1-\epsilon)x^2],$$
$$U=-(1+\epsilon)y, \quad V=(1-\epsilon)x. \tag{A2}$$

Here, the operator L_z denotes the stratification effect and it contains a second-order differentiation, with respect to z. Its detailed expression is not required in the following discussions.

Let us consider the linear stability of the above steady state. The perturbation is assumed to have the form

$$\psi'=\hat{\psi}(x,y,t)f(z), \tag{A3}$$

with $f(z)$ being an eigenfunction of the Sturm–Liouville problem associated with the operator L_z and suitable boundary conditions:

$$L_z f(z)=-\lambda^2 f(z). \tag{A4}$$

Assuming that $\hat{\psi}(x,y,t)$ has the form of a plane wave

$$\hat{\psi}(x,y,t)=A(\varphi)e^{i(k_1x+k_2y)},$$
$$k_1=\cos\varphi, \quad k_2=\sqrt{\frac{1+\epsilon}{1-\epsilon}}\sin\varphi, \tag{A5}$$
$$\varphi=\sqrt{(1+\epsilon)(1-\epsilon)}\,t,$$

we obtain the equation describing the time evolution of $A(\varphi)$:

$$\frac{d}{d\varphi}\left[\left(\lambda^2+\frac{1-\epsilon\cos\varphi}{1-\epsilon}\right)A\right]=0. \tag{A6}$$

It is easily solved to yield

$$\left(\lambda^2+\frac{1-\epsilon\cos\varphi}{1-\epsilon}\right)A=\text{const}, \tag{A7}$$

indicating that there is no elliptical instability, since the coefficient in front of $A(\varphi)$ is positive definite. This result is consistent with the observation in the main text, that the growth rate of the instability decreases rapidly as the parameters N and Ro are increased.

[1]R. T. Pierrehumbert, "Universal short-wave instability of two-dimensional eddies in an inviscid fluid," Phys. Rev. Lett. **57**, 2157 (1986).
[2]B. J. Bayly, "Three-dimensional instability of elliptical flow," Phys. Rev. Lett. **57**, 2160 (1986).
[3]F. Waleffe, "On the three-dimensional instability of strained vortices," Phys. Fluids A **2**, 76 (1990).
[4]C. Y. Tsai and S. E. Widnall, "The stability of short waves on a straight vortex filament in a weak externally imposed strain field," J. Fluid Mech. **73**, 721 (1976).
[5]D. W. Moore and P. G. Saffman, "The instability of a straight vortex filament in a strain field," Proc. R. Soc. London Ser. A **346**, 415 (1975).
[6]Ye. B. Gledzer, F. V. Dolzhanskiy, A. M. Obukhov, and V. M. Ponomarev, "An experimental and theoretical study of the stability of motion of a liquid in an elliptical cylinder," Izv. Atmos. Oceanic Phys. **11**, 981 (1975).
[7]W. V. R. Malkus and F. Waleffe, "Transition from order to disorder in elliptical flow: a direct path to shear flow turbulence," in *Advances in Turbulence 3*, Proceedings of the 3rd European Turbulence Conference (Springer-Verlag, New York, 1991), p. 197.
[8]S. E. Widnall, D. B. Bliss, and C. Y. Tsai, "The instability of short waves on a vortex ring," J. Fluid Mech. **66**, 35 (1974).
[9]E. B. Gledzer and V. M. Ponomarev, "Instability of bounded flows with elliptical streamlines," J. Fluid Mech. **240**, 1 (1992).
[10]M. J. Landman and P. G. Saffman, "The three-dimensional instability of strained vortices in a viscous fluid," Phys. Fluids **30**, 2339 (1987).
[11]S. A. Orszag and A. Patera, "Secondary instability of wall-bounded shear flows," J. Fluid Mech. **128**, 347 (1983).
[12]A. D. D. Craik, "The stability of unbounded two- and three-dimensional flows subject to body forces: some exact solutions," J. Fluid Mech. **198**, 275 (1989).
[13]T. Miyazaki and Y. Fukumoto, "Three-dimensional instability of strained vortices in a stably stratified fluid," Phys. Fluids A **4**, (1992).
[14]A. Lifschitz, "Short wavelength instabilities of incompressible three-dimensional flows and generation of vorticity," Phys. Lett. A **157**, 481 (1991).
[15]A. Lifschitz and E. Hameiri, "Local stability conditions in fluid dynamics," Phys. Fluids A **3**, 2644 (1991).
[16]T. Miyazaki, "Parametric excitation of buoyancy oscillation and formation of internal boundary layers in a stably stratified fluid," Phys. Fluids A **4**, 2145 (1992).
[17]A. D. D. Craik and W. O. Criminale, "Evolution of wavelike disturbances in shear flows: a class of exact solutions of the Navier–Stokes equations," Proc. R. Soc. London Ser. A **406**, 13 (1986).